

Performance enhancement of high-speed free space optical transmission link for the implementation of 5G and internet of things

Duong Huu Ai^{1,3}, Van Loi Nguyen², Khanh Ty Luong², Viet Truong Le²

¹Faculty of Computer Engineering and Electronics, The University of Danang - Vietnam-Korea University of Information and Communication Technology, Danang, Vietnam

²Faculty of Computer Science, The University of Danang - Vietnam-Korea University of Information and Communication Technology, Danang, Vietnam

³Digital Science and Technology Institute, The University of Danang - Vietnam-Korea University of Information and Communication Technology, Danang, Vietnam

Article Info

Article history:

Received Mar 1, 2024

Revised Jul 14, 2024

Accepted Aug 6, 2024

Keywords:

Average channel capacity

Free-space optical

communications

Gamma-Gamma distribution

Misalignment fading effects

Reconfigurable intelligent

surfaces

ABSTRACT

Internet of things (IoT) with continuous development allows multiple devices to be connected to each other through the external environment. With that, free space optical (FSO) transmission links provide high data transmission rates, so that enhanced quality of services, that is very suitable for deployment for fifth generation (5G) and IoT. FSO is known as license free, cost effective and line-of-sight green communication technology, which is employed in various circumstances, such as high data rate connections between buildings within campus or city. This study performs enhancement of FSO link for reconfigurable intelligent surfaces (RISs) aided over free space with gamma-gamma distribution channels. The paper analyzes the performance of FSO links affected by misalignment fading, RISs aided, and link distance with the subcarrier quadrature amplitude modulation scheme. Several numerical outcomes obtained for average electrical end-to-end signal-to-noise ratio, misalignment fading displacement standard deviation and link distance are shown to illustrate the average channel capacity of systems.

This is an open access article under the [CC BY-SA](#) license.



Corresponding Author:

Duong Huu Ai

Faculty of Computer Engineering and Electronics, The University of Danang - Vietnam-Korea University of Information and Communication Technology

Danang, Vietnam

Email: dhai@vku.udn.vn

1. INTRODUCTION

With the advantage of optical wireless communication (OWC), that it is used for the specialized environments and high data transmission rates link requirements of the fifth-generation wireless communication and beyond [1]. The benefits of free space optical links are larger bandwidth, cost effectiveness, higher channel capacity, setup and system design are also uncomplicated [1]–[5]. However, there are challenges as optical wavelengths propagate through the free space, such as signal obstruction, attenuation, signal fading and misalignment fading [6]–[10]. This paper performs enhancement free space optical (FSO) link to solve performance of systems affected with using reconfigurable intelligent surfaces (RISs) technique over strong atmospheric turbulence. RISs is relay technique that is considered to have many benefits and has been studied in recent years [11]–[15].

Over the years, there have been many studies on optical wireless communication using RISs technology and the results show its superiority. However, the channel state parameters have not been combined and fully evaluated, and average channel capacity (ACC), quadrature amplitude modulation (QAM) technique unused [16]–[21]. RISs technique offers optical wireless communication link many benefits over relay technique of systems, these benefits of RISs have been recently studied in [22]–[26].

This paper, we performance enhancement of high-speed free space optical link for the implementation of 5G and beyond using RISs over gamma-gamma distribution. The paper is organized as follows. Section 2 presents the system and channel models. Section 3 presents the average channel capacity calculation. Section 4 describes numerical results and discussions, and in section 5, the paper concludes.

2. SYSTEM AND CHANNEL MODELS

2.1. System model

The system and channel model for performing the evaluation is describe in Figure 1, in which, the optical signal transmitted from transmitter node S to receiver node D will be reflected at RISs. Due to obstructions, the signal does not transmit directly from S to D and the RISs is placed in the appropriate location and acts as a complete reflector of the optical signal, the signal absorption is negligible. In this case, the transmission channel is affected by strong turbulence of weather and is modeled by gamma-gamma distribution.

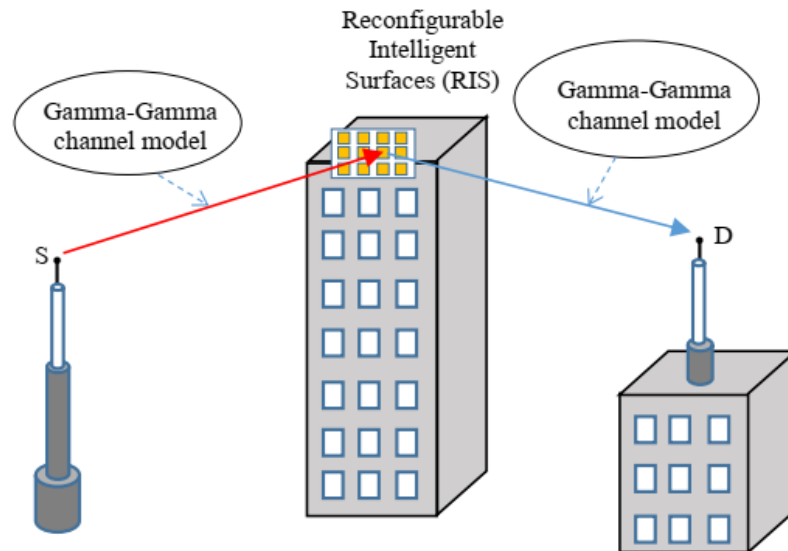


Figure 1. The system and channel model with RISs aided

The factors characterizing a free space optical channel comprises the atmospheric attenuation (h_l), atmospheric turbulence (h_a), and misalignment fading (h_p). The channel state model (h) is composed of three elements, and it is given by (1).

$$h = h_l \times h_a \times h_p \quad (1)$$

In this case, the transmission channel is affected by moderate to strong turbulence of weather and gamma-gamma distribution is used, the pdf of irradiance intensity of optical signal [18], $f_{h_a}(h_a)$, it is expressed by (2).

$$f_{h_a}(h_a) = \frac{2(\alpha\beta)^{\frac{\alpha+\beta}{2}}}{\Gamma(\alpha)\Gamma(\beta)} h_a^{\frac{\alpha+\beta}{2}-1} K_{\alpha-\beta}(2\sqrt{\alpha\beta h_a}) \quad (2)$$

where $K_{\alpha-\beta}(\cdot)$ is the modified Bessel function, $\Gamma(\alpha)$, $\Gamma(\beta)$ is the Gamma function, β is positive parameter represents of small-scale cells, α represents of large-scale cells of the scattering process.

$$\alpha = \left[\exp \left(\frac{0.49\sigma_2^2}{(1+0.18d^2+0.56\sigma_2^{12/5})^{7/6}} \right) - 1 \right]^{-1} \quad (3)$$

$$\beta = \left[\exp \left(\frac{0.51\sigma_2^2(1+0.69\sigma_2^{12/5})^{-5/6}}{1+0.9d^2+0.62\sigma_2^{12/5}} \right) - 1 \right]^{-1} \quad (4)$$

In (3) and (4), $d = \sqrt{kD^2/4L}$, where $k = 2\pi/\lambda$ is the wave number, λ is the optical wavelength, D is the radius of receiving aperture, L is the link distance, and σ_2 is the Rytov variance, $\sigma_2^2 = 0.492C_n^2k^{7/6}L^{11/6}$, where C_n^2 is the structure parameter of refractive-index.

The atmospheric attenuation (h_l) is always present factor when signal transmitted in the air, the value can be determined in each given environment, and it is described by the Beer-Lambert's law, it is expressed by (5).

$$h_l = \exp(-\sigma_l L_a) \quad (5)$$

where, L_a is the distance of channel, σ_l is the attenuation coefficient, the attenuation coefficient is a measure of how much a wave or signal decreases in intensity as it travels through a medium, the attenuation coefficient σ_l with the value of σ_l (dB) [dB/km], it is given by (6).

$$\sigma_l = \frac{3.91}{V[\text{km}]} \left(\frac{\lambda[\text{nm}]}{550} \right)^{-q} \quad (6)$$

where, q is the size distribution of scattering particles, V is the visibility. The pdf of misalignment fading model, $f_{h_p}(h_p)$ [15], it is given by (7).

$$f_{h_p}(h_p) = \frac{\xi^2}{A_0 \xi^2} h_p^{\xi^2-1}, \quad 0 \leq h_p \leq A_0 \quad (7)$$

where, $A_0 = [\text{erf}(v)]^2$ is power at radial distance $z = 0$, $v = \sqrt{\pi}r/(\sqrt{2}\omega_z)$, r , ω_z are aperture radius and beam waist at the distance z , respectively, ω_{zeq} can calculated by (8).

$$\omega_{zeq} = \omega_z(\sqrt{\pi} \text{erf}(v)/2v \times \exp(-v^2))^{1/2} \quad (8)$$

where, $\omega_z = \omega_0[1 + \varepsilon(\lambda L/\pi\omega_0^2)^2]^{1/2}$, at $z = 0$, the transmitter beam waist radius is ω_0 , $\varepsilon = (1 + 2\omega_0^2)/\rho_0^2$ and $\rho_0 = (0.55C_n^2k^2L)^{-3/5}$ is the coherence length.

2.2. The signal-to-noise ratio

Assume that, the RISs module is placed in the appropriate location and acts as a complete reflector of the optical signal, the signal absorption is negligible, and take over the channel phases perfect knowledge at RISs and transmitter node S. The detected signal at receiver node D [19] is expressed by (9).

$$y = \sqrt{E_s}(h\mu e^{j\theta}g)x + n \quad (9)$$

where, E_s is the symbol energy, h and g are respectively the transmitter node S to RISs and RISs to receiver D complex channel vectors, it is expressed by (10).

$$\gamma = \bar{\gamma}|h\mu e^{j\theta}g|^2 \quad (10)$$

where $\bar{\gamma} = \frac{E_s}{N_0}$ represents the average electrical signal-to-noise ratio in both from transmitter node S to RISs and RISs to receiver D, N_0 is the noise power spectral density.

2.3. The PDF of signal-to-noise ratio

The probability density function of average electrical SNR of system, $f_\gamma(\gamma)$, is computed from the SNRs, γ_h , and γ_g . The gain of system is expressed by $h\mu e^{j\theta}g$, where $\mu e^{j\theta}$ is deterministic in contrast to h and g . The PDF of average electrical SNR, $f_\gamma(\gamma)$, is evaluated in [20] and it is expressed by (11).

$$f_Y(\gamma) = \int_0^\infty f_{\gamma_h}(t) f_{\gamma_g}\left(\frac{\gamma}{t}\right) \frac{1}{t} dt \quad (11)$$

where $f_{\gamma_h}(\cdot)$ is the PDF of the S to RIS, and $f_{\gamma_g}(\cdot)$ is the RIS to D channels. A combined distribution including strong atmospheric turbulence, misalignment fading, and atmospheric attenuation. The PDF of channel state, $f_{\gamma_i}(\gamma_i)$ is expressed as (12),

$$f_{\gamma_i}(\gamma_i) = \frac{\xi^2}{(A_0 X_i)^{\xi^2} \Gamma(\alpha) \Gamma(\beta)} \times G_{1,3}^{2,1} \left[\alpha \beta \frac{\gamma_i}{A_0 X_i \bar{\gamma}} \mid \alpha, \beta, \xi^2 \right] \quad (12)$$

Perform transformation γ_i by t and $\frac{\gamma}{t}$ in (12), and obtain $f_{\gamma_h}(t)$ and $f_{\gamma_g}\left(\frac{\gamma}{t}\right)$ respectively as (13) and (14).

$$f_{\gamma_h}(t) = \frac{\xi^2}{(A_0 X_i)^{\xi^2} \Gamma(\alpha) \Gamma(\beta)} \times G_{1,3}^{2,1} \left[\alpha \beta \frac{t}{A_0 X_i \bar{\gamma}_h} \mid \alpha, \beta, \xi^2 \right] \quad (13)$$

$$f_{\gamma_g}\left(\frac{\gamma}{t}\right) = \frac{\xi^2}{(A_0 X_i)^{\xi^2} \Gamma(\alpha) \Gamma(\beta)} \times G_{1,3}^{2,1} \left[\alpha \beta \frac{\gamma}{A_0 X_i \bar{\gamma}_g t} \mid \alpha, \beta, \xi^2 \right] \quad (14)$$

In (13) and (14), $\bar{\gamma}_h$ and $\bar{\gamma}_g$ are average values of the γ_h and γ_g , respectively. Perform substitute (13) and (14) in to (11), the pdf of average electrical SNR, $f_Y(\gamma)$, is given as (15).

$$f_Y(\gamma) = \frac{\xi^4}{(X_i A_0)^{\xi^4} (\Gamma(\alpha) \Gamma(\beta))^2} \times \int_0^\infty G_{1,3}^{2,1} \left[\alpha \beta \frac{t}{A_0 X_i \bar{\gamma}_h} \mid \alpha, \beta, \xi^2 \right] \times G_{1,3}^{2,1} \left[\alpha \beta \frac{\gamma}{A_0 X_i \bar{\gamma}_g t} \mid \alpha, \beta, \xi^2 \right] \frac{1}{t} dt \quad (15)$$

With the integral of two function Meijer, perform the solution of the integral function in (15), and obtain the exact PDF of average electrical SNR, the exact unified PDF, $f_Y(\gamma)$, as (16).

$$f_Y(\gamma) = \frac{\xi^4}{(X_i A_0)^{\xi^4} (\Gamma(\alpha) \Gamma(\beta))^2} \times H_{2,6}^{4,2} \left(\frac{(\alpha \beta)^2 \gamma}{(A_0 X_i)^2 \bar{\gamma}_h \bar{\gamma}_g} \mid (1 + \xi^2, 1), (1 - \alpha, -1), (1 - \beta, -1), (1 - \xi^2, -1) \right) \quad (16)$$

$$\left(\alpha, 1, (\beta, 1), (-\xi^2, -1), (\xi^2, 1) \right)$$

3. AVERAGE CHANNEL CAPACITY CALCULATION

The channel capacity as a random variable, known as average channel capacity (ACC), $\langle \bar{C} \rangle$, the average spectral efficiency (ASE) in bits/s/Hz can also be described in terms of ACC. Assuming that, the optical channel is memoryless, ergodic, stationary with perfect channel state information and turbulence statistics is available at both the transmitters and receivers [18]. The ASE can be estimated as (17).

$$\langle \bar{C} \rangle = \int_0^\infty B \log_2(1 + \gamma) \times f(\gamma) d\gamma, \text{ [bit/s/Hz]} \quad (17)$$

where B is the bandwidth of transmission channel, $f_Y(\gamma)$ is the pdf of SNR. In (17), using the equality $\ln(1 + x) = \sum_{k=1}^{+\infty} (-1)^{k+1} x^k / k$ for $0 \leq x \leq 1$. The pdf of SNR is respectively described in Gamma-Gamma is expressed as (18).

$$\langle \bar{C} \rangle = \int_0^\infty \frac{\xi^4 \sum_{k=1}^{+\infty} \frac{(-1)^{k+1} \gamma^k}{k}}{\ln(2) (X_i A_0)^{\xi^4} (\Gamma(\alpha) \Gamma(\beta))^2} \quad (18)$$

$$H_{2,6}^{4,2} \left(\frac{(\alpha \beta)^2 \gamma}{(A_0 X_i)^2 \bar{\gamma}_h \bar{\gamma}_g} \mid (1 + \xi^2, 1), (1 - \alpha, -1), (1 - \beta, -1), (1 - \xi^2, -1) \right) d\gamma$$

$$\left(\alpha, 1, (\beta, 1), (-\xi^2, -1), (\xi^2, 1) \right)$$

4. NUMERICAL RESULTS AND DISCUSSION

In this part, we show numerical results for ASE analysis of the transmission link with RIS aided from (16) and (18), and analyze the performance influenced by misalignment fading, radius of a circular receiving aperture, and link distance for the subcarrier quadrature amplitude modulation technique. The constants and parameters considered in our analysis are presented in Table 1.

Table 1. System constants and parameters

Parameter	Symbol	Value
Laser wavelength	λ	1550 nm
Modulation index	κ	1
Total noise variance	N_0	10^{-7} A/Hz
Photodetector responsivity	\mathfrak{R}	1 A/W
Structure parameter of refractive-index	C_n^2	$3.10^{-14} m^{-2/3}$
Receiver aperture diameter	D	0.08m

Figure 2 illustrates the ASE for FSO link with RIS aided and without RIS aided respect to $\bar{\gamma}$, for various values of displacement standard deviation, σ_s , and distances of transmission channel, $L = 2000$ m. It can be seen that, the average spectral efficiency strongly depends on the RISs aided, since the great value domain of SNR is the stronger effects of RIS becomes. Obviously, with longer link distance, the misalignment fading effects on ASE is greater. It has been noticed that when the without RIS aided, the average channel capacity of the system degrades.

Figure 3 illustrate the ASE performance versus link distance for various values of misalignment fading displacement standard deviation in case with RIS and without RIS. It is clearly proven that; the ASE performance is deteriorated significantly when link distance increase and the average spectral efficiency performance is increase significantly with the RIS aided. In brief, the ASE strongly relies on the misalignment fading displacement standard deviation and reconfigurable intelligent surfaces.

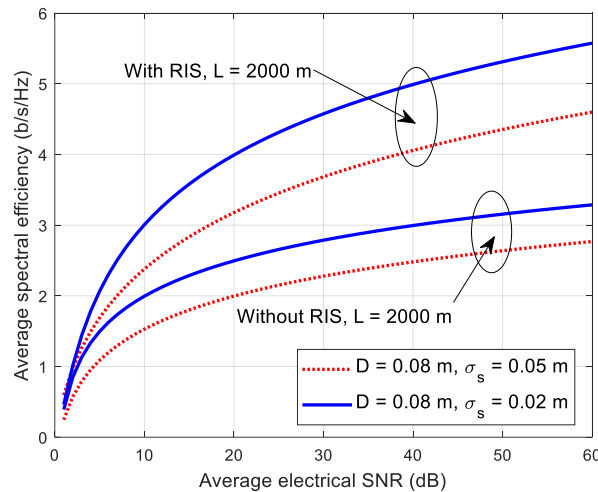


Figure 2. Average spectral efficiency performance versus average electrical SNR for various values of σ_s

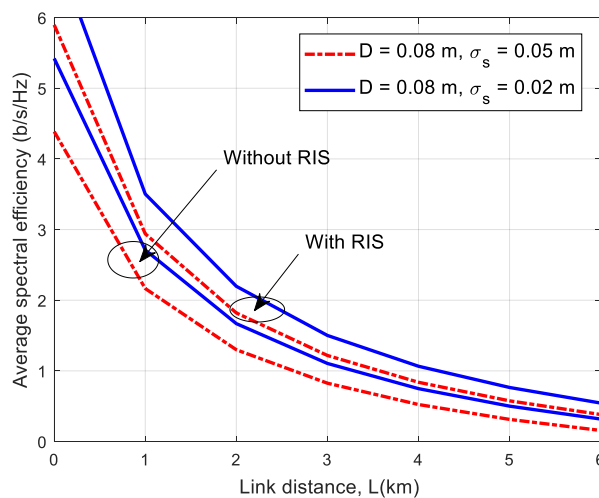


Figure 3. Average spectral efficiency performance versus link distance for various values of σ_s

5. CONCLUSION

This study, we introduced the performance analysis of the high-speed FSO transmission link over strong turbulence of weather channels model by the gamma-gamma distributions that used to describe the fluctuation of the optical propagation. We studied the average spectral efficiency of the system in different link distance, misalignment fading displacement standard deviation and reconfigurable intelligent surfaces. The numerical results proved that, regardless the link distance and misalignment fading, the average spectral efficiency improves significantly with the support of reconfigurable intelligent surfaces.

REFERENCES

- [1] Y. Kaymak, R. Rojas-Cessa, J. Feng, N. Ansari, M. Zhou, and T. Zhang, "A survey on acquisition, tracking, and pointing mechanisms for mobile free-space optical communications," *IEEE Communications Surveys and Tutorials*, vol. 20, no. 2, pp. 1104–1123, 2018, doi: 10.1109/COMST.2018.2804323.
- [2] M. Z. Chowdhury, M. Shahjalal, S. Ahmed, and Y. M. Jang, "6G wireless communication systems: applications, requirements, technologies, challenges, and research directions," *IEEE Open Journal of the Communications Society*, vol. 1, pp. 957–975, 2020, doi: 10.1109/OJCOMS.2020.3010270.
- [3] H. A. Duong, V. L. Nguyen, and K. T. Luong, "Misalignment fading effects on the ACC performance of relay-assisted MIMO/FSO systems over atmospheric turbulence channels," *International Journal of Electrical and Computer Engineering*, vol. 12, no. 1, pp. 966–973, Feb. 2022, doi: 10.11591/ijece.v12i1.pp966-973.
- [4] K. O. Odeyemi and P. A. Owolawi, "On the performance of energy harvesting AF partial relay selection with TAS and outdated channel state information over identical channels," *International Journal of Electrical and Computer Engineering*, vol. 10, no. 5, pp. 5296–5305, Oct. 2020, doi: 10.11591/ijece.v10i5.pp5296-5305.
- [5] D. H. Ai, D. T. Dang, Q. H. Dang, and T. Le Kim, "Analysis on the performance of pointing error effects for RIS-aided FSO link over gamma-gamma channels," *TELKOMNIKA (Telecommunication Computing Electronics and Control)*, vol. 21, no. 4, pp. 718–724, Aug. 2023, doi: 10.12928/telkomnika.v21i4.24537.
- [6] M. Najafi and R. Schober, "Intelligent reflecting surfaces for free space optical communication," in *2019 IEEE Global Communications Conference (GLOBECOM)*, Dec. 2019, pp. 1–7, doi: 10.1109/GLOBECOM38437.2019.9013840.
- [7] D. H. Ai, V. L. Nguyen, H. H. Duc, and K. T. Luong, "On the performance of reconfigurable intelligent surface-assisted UAV-to-ground communication systems," *TELKOMNIKA (Telecommunication Computing Electronics and Control)*, vol. 21, no. 4, pp. 736–741, Aug. 2023, doi: 10.12928/telkomnika.v21i4.24720.
- [8] L. Yang, W. Guo, D. B. da Costa, and M.-S. Alouini, "Free-space optical communication with reconfigurable intelligent surfaces," *arXiv:2012.00547*, Nov. 2020.
- [9] H. Wang, Z. Zhang, B. Zhu, J. Dang, and L. Wu, "Two new approaches to optical IRSs: schemes and comparative analysis," *arXiv:2012.15398*, Dec. 2020.
- [10] A. R. Ndjongue, T. M. N. Ngatched, O. A. Dobre, and H. Haas, "Design of a power amplifying-RIS for free-space optical communication systems," *arXiv: 2104.03449*, Apr. 2021.
- [11] M. Zeng, X. Li, G. Li, W. Hao, and O. A. Dobre, "Sum rate maximization for IRS-assisted uplink NOMA," *IEEE Communications Letters*, vol. 25, no. 1, pp. 234–238, Jan. 2021, doi: 10.1109/lcomm.2020.3025978.
- [12] M. A. ElMossallamy, H. Zhang, L. Song, K. G. Seddik, Z. Han, and G. Y. Li, "Reconfigurable intelligent surfaces for wireless communications: principles, challenges, and opportunities," *IEEE Transactions on Cognitive Communications and Networking*, vol. 6, no. 3, pp. 990–1002, Sep. 2020, doi: 10.1109/tccn.2020.2992604.
- [13] S. Atapattu, R. Fan, P. Dharmawansa, G. Wang, J. Evans, and T. A. Tsiftsis, "Reconfigurable intelligent surface assisted two-way communications: performance analysis and optimization," *IEEE Transactions on Communications*, vol. 68, no. 10, pp. 6552–6567, Oct. 2020, doi: 10.1109/tcomm.2020.3008402.
- [14] E. Basar, "Reconfigurable intelligent surface-based index modulation: a new beyond MIMO paradigm for 6G," *IEEE Transactions on Communications*, vol. 68, no. 5, pp. 3187–3196, May 2020, doi: 10.1109/tcomm.2020.2971486.
- [15] D. H. Ai, C. D. Vuong, and D. T. Dang, "Average symbol error rate analysis of reconfigurable intelligent surfaces-assisted free-space optical link over log-normal turbulence channels," *International Journal of Electrical and Computer Engineering*, vol. 13, no. 1, pp. 571–578, Feb. 2023, doi: 10.11591/ijece.v13i1.pp571-578.
- [16] D. Wang, C. Watkins, and H. Xie, "MEMS mirrors for LiDAR: a review," *Micromachines*, vol. 11, no. 5, p. 456, Apr. 2020, doi: 10.3390/mi11050456.
- [17] C. U. Hail, A. U. Michel, D. Poulidakos, and H. Eghlidi, "Optical metasurfaces: evolving from passive to adaptive," *Advanced Optical Materials*, vol. 7, no. 14, May 2019, doi: 10.1002/adom.201801786.
- [18] D. H. Ai, H. D. Trung, and D. T. Tuan, "On the ASER performance of amplify-and-forward relaying MIMO/FSO systems using SC-QAM signals over log-normal and gamma-gamma atmospheric turbulence channels and pointing error impairments," *Journal of Information and Telecommunication*, vol. 4, no. 3, pp. 267–281, Jul. 2020, doi: 10.1080/24751839.2020.1732734.
- [19] Z. Yigit, E. Basar, and I. Altunbas, "Low complexity adaptation for reconfigurable intelligent surface-based MIMO systems," *IEEE Communications Letters*, vol. 24, no. 12, pp. 2946–2950, Dec. 2020, doi: 10.1109/lcomm.2020.3014820.
- [20] L. Yang, F. Meng, J. Zhang, M. O. Hasna, and M. Di Renzo, "On the performance of RIS-assisted dual-hop UAV communication systems," *IEEE Transactions on Vehicular Technology*, vol. 69, no. 9, pp. 10385–10390, 2020, doi: 10.1109/TVT.2020.3004598.
- [21] T. Ma, Y. Xiao, X. Lei, P. Yang, X. Lei, and O. A. Dobre, "Large intelligent surface assisted wireless communications with spatial modulation and antenna selection," *IEEE Journal on Selected Areas in Communications*, vol. 38, no. 11, pp. 2562–2574, Nov. 2020, doi: 10.1109/jsac.2020.3007044.
- [22] J. Ye, S. Guo, and M.-S. Alouini, "Joint reflecting and precoding designs for SER minimization in reconfigurable intelligent surfaces assisted MIMO systems," *IEEE Transactions on Wireless Communications*, vol. 19, no. 8, pp. 5561–5574, Aug. 2020, doi: 10.1109/twc.2020.2994455.
- [23] H. Wang *et al.*, "Performance of wireless optical communication with reconfigurable intelligent surfaces and random obstacles," *arXiv:2001.05715*, Jan. 2020.
- [24] L. Yang, F. Meng, Q. Wu, D. B. da Costa, and M.-S. Alouini, "Accurate closed-form approximations to channel distributions of RIS-aided wireless systems," *IEEE Wireless Communications Letters*, vol. 9, no. 11, pp. 1985–1989, Nov. 2020, doi: 10.1109/lwc.2020.3010512.

- [25] M. Di Renzo, A. Guidotti, and G. E. Corazza, "Average rate of downlink heterogeneous cellular networks over generalized fading channels: a stochastic geometry approach," *IEEE Transactions on Communications*, vol. 61, no. 7, pp. 3050–3071, Jul. 2013, doi: 10.1109/tcomm.2013.050813.120883.
- [26] M. Di Renzo, M. Iezzi, and F. Graziosi, "On diversity order and coding gain of multisource multirelay cooperative wireless networks with binary network coding," *IEEE Transactions on Vehicular Technology*, vol. 62, no. 3, pp. 1138–1157, Mar. 2013, doi: 10.1109/tvt.2012.2229476.

BIOGRAPHIES OF AUTHORS



Duong Huu Ai    he received the master of electronic engineering from Danang University of Technology, Vietnam, in 2011, and the Ph.D. degree in electronics and telecommunications from Hanoi University of Technology, Vietnam, in 2018. Currently, he is a lecturer at The University of Danang - Vietnam-Korea University of Information and Communication Technology, Danang City, Vietnam. His research interests include optical wireless communications, optical and quantum electronics, 5G wireless communications and broadband networks, and IoT. He can be contacted at email: dhai@vku.udn.vn.



Van Loi Nguyen    he received his master of engineering in computer science from the University of Danang, Vietnam in 2010, a Ph.D. degree from Soongsil University in 2017. Currently, he is a lecturer at The University of Danang - Vietnam-Korea University of Information and Communication Technology, Danang City, Vietnam. His research interests include multimedia, information retrieval, artificial intelligence, database, and IoT. He can be contacted at email: nvloi@vku.udn.vn.



Khanh Ty Luong    he received his master of engineering in computer science from the University of Danang, Vietnam in 2012. Currently, he is a lecturer at The University of Danang - Vietnam-Korea University of Information and Communication Technology, Danang City, Vietnam. His research interests include database, artificial intelligence, IoT, and optical wireless communications. He can be contacted email: lkty@vku.udn.vn.



Viet Truong Le    He received his master of science in informatics from Hue University, Vietnam in 2005. Currently, he is a lecturer at The University of Danang - Vietnam-Korea University of Information and Communication Technology, Danang City, Vietnam. His research interests include database, data warehouse, data mining, system analysis and design. He can be contacted at email: lvtruong@vku.udn.vn.